

# A LATTICE MODEL FOR LLT POLYNOMIALS

MICHAEL CURRAN<sup>1</sup>, CALVIN YOST-WOLFF<sup>2</sup>, SYLVESTER W. ZHANG<sup>3</sup>,  
AND VALERIE ZHANG<sup>4</sup>

ABSTRACT. We construct a family of 2 dimensional lattice models depending on a positive integer  $n$  whose partition functions are equal to the LLT polynomials of Lascoux, Leclerc and Thibon (originally named  $n$ -ribbon Schur functions). We conjecture that our lattice model is solvable for all  $n$ , and compute the Yang-Baxter equations for up to  $n = 3$ .

## CONTENTS

1. Introduction	1
2. Background on Tableaux and Symmetric Functions	3
3. Lattice Models	6
4. Proof of Theorem 3.5	12
5. Exact Solvability	15
6. Future Directions	16
References	16
A. Yang-Baxter Equation for 2, 3-Ribbon Lattice Models	17

## 1. INTRODUCTION

The study of symmetric functions is of great importance, and has given rise to many interesting discoveries in combinatorics, algebraic geometry, and representation theory in recent years. There has also been a strong interest in  $q$ -analogues and  $q, t$ -analogues of symmetric functions. For example, Lascoux, Leclerc, and Thibon's LLT polynomials [LLT97] are  $q$ -analogs of products of the well known Schur functions, and have led to the discovery of many interesting results in symmetric function theory. Many other families of symmetric functions  $\{F_\lambda(x_1, x_2, \dots) : \lambda \in S\}$  over a field  $K$  with index set  $S$  satisfy three important properties:

- (1) They are generating functions for a set of nice tableaux

$$F_\lambda(x_1, x_2, \dots) = \sum_T s(T)x^{\text{wt}(T)}, \quad (1)$$

where the sum is taken over all tableaux of shape  $\lambda$ . The composition  $\text{wt}(T)$  is usually called the *weight* of  $T$  and  $s(T)$  is some other statistic of  $T$  taking values in  $K$ .

---

<sup>1</sup>Williams College.

<sup>2</sup>Massachusetts Institute of Technology.

<sup>3</sup>University of Minnesota, Twin Cities.

<sup>4</sup>Harvard University.

- (2) Along with a related dual family  $\{G_\lambda(x_1, x_2, \dots) : \lambda \in S\}$  of symmetric functions, they satisfy a Cauchy identity

$$\sum_{\lambda \in S} F_\lambda(x_1, x_2, \dots) G_\lambda(y_1, y_2, \dots) = \prod_{i,j=1}^{\infty} \sum_{k=0}^{\infty} b_k x_i^k x_j^k, \quad (2)$$

where  $b_k$  is a set of parameters in  $K$ .

- (3) They satisfy a Pieri identity

$$h_k(x_1, x_2, \dots) F_\lambda(x_1, x_2, \dots) = \sum_{\mu \rightarrow_k \lambda} b_{\lambda, \mu} F_\mu(x_1, x_2, \dots), \quad (3)$$

where  $k$  is a positive integer,  $\{h_1, h_2, \dots\}$  is a set of symmetric polynomials over  $K$ , and  $b_{\lambda, \mu} \in K$  are coefficients for each  $\lambda, \mu$  satisfying some condition  $\mu \rightarrow_k \lambda$ .

In most cases  $K$  is either  $\mathbb{Q}$  or  $\mathbb{Q}(q)$ . The simplest family satisfying these three conditions is the family of Schur functions. In this case,  $S$  is the set of partitions, the tableaux of interest are the semistandard Young tableaux,  $s(T)$  is 1, and  $\text{wt}(T)$  is the usual weight of a Young tableaux. In the Cauchy identity, the dual family is also equal to the Schur functions, and all of the coefficients  $b_i$  are equal to 1. Finally, for the Pieri rule, the  $h_k$  are the homogeneous symmetric functions, the condition  $\mu \rightarrow_k \lambda$  is that  $\lambda/\mu$  is a horizontal strip of size  $k$ , and all the coefficients  $b_{\lambda, \mu}$  are equal to 1. The LLT polynomials are another example of a family of symmetric functions satisfying these three properties. In [Lam05a], it was shown that certain representations of Heisenberg algebras give rise to families of symmetric function, including the Schur and LLT polynomials, satisfying these three properties. This relation between representation theory of Heisenberg algebras and families of symmetric functions is known as the combinatorial Boson-Fermion correspondence.

In the case of Schur functions, the Heisenberg algebra representation can be viewed directly as a lattice model [BBF09] and this viewpoint leads to nice combinatorial proofs of these three identities. These lattice models are intimately related with a multitude of combinatorial objects including semistandard Young tableaux, non-intersecting lattice paths, and free fermionic operators [ZJ09]. For other families of polynomials satisfying equations (1) to (3), including the LLT polynomials, however, it was not thought that there was a corresponding lattice model related to the family, and all the identities known about the LLT polynomials arose from algebraic methods using representation theory of infinite dimensional lie algebras or the quantum affine algebra  $U_q(\widehat{\mathfrak{sl}}_n)$  [Lam05b].

In our work, we construct a 2 dimensional lattice model depending on an integer  $n$ , which we call an  $n$ -ribbon lattice which naturally gives rise to the LLT polynomials. It can be thought of as a generalization of the square ice model [Bax89]. The north and south entries of a vertex are decorated by  $\{+, -\}$ , and the east and west entries of a vertex are decorated by  $\{+, -\}^n$ , i.e.  $n$ -tuples of  $+$  and  $-$  (figure 1 left). In light of conditions we will specify later for a vertex to be admissible, we depict the horizontal edge of a vertex as multiple intertwining edges (figure 1 right) that are decorated by  $+$  and  $-$ . More often in the paper we shall use arrows to decorate a lattice model, in which case  $+$  will be identified with left and up arrows and  $-$  will be identified with right and down arrows. A detailed description of our lattice model will be given in section 3.2. The  $n = 1$  case is a 5-vertex model which is very similar to a six vertex model of Brubaker-Bump-Friedberg [BBF09].

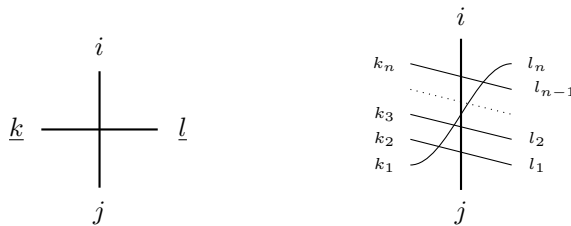


FIGURE 1. **Left:** A vertex of a  $n$ -ribbon lattice, where  $i, j \in \{+, -\}$ ,  $\underline{k} = (k_1, \dots, k_n) \in \{+, -\}^n$  and  $\underline{l} = (l_1, \dots, l_n) \in \{+, -\}^n$ . **Right:** admissible  $n$ -ribbon vertex with intertwining horizontal edges.

We demonstrate that the  $n$ -ribbon lattice model is *exactly solvable* (or *integrable*), meaning that it satisfies an appropriate Yang-Baxter equation [Bax89] for  $n = 1, 2$  and  $3$  through direct computation. This solvability implies that the LLT polynomials are indeed symmetric. In general, Yang-Baxter equations are indispensable tools in statistical mechanics, used to compute partition functions, to detect more complicated symmetries, and to make connections with quantum groups.

The plan of the paper is as follows. In section 2 we review the background in tableaux and symmetric functions, and define our main object of interest: the LLT polynomials. In section 3, we discuss a 5-vertex model whose partition functions are Schur polynomials, and then generalize this 5-vertex model to what we call  $n$ -ribbon lattice model, whose partition functions give rise to the  $n$ -LLT polynomials. In section 4 we demonstrate a weight-preserving bijection from our lattice model to the set of semi-standard ribbon tableaux, thereby proving our main result. In section 5 we discuss the solvability (Yang-Baxter equation) of our lattice model and we end our paper in section 6 with a discussion of future research directions.

**Acknowledgements.** This research was carried out as part of the 2019 Combinatorics REU program at the School of Mathematics of the University of Minnesota, Twin Cities supported by NSF RTG grant DMS-1148634. The authors would like to thank Ben Brubaker, Claire Frchette and Katy Weber for their mentorship and guidance.

## 2. BACKGROUND ON TABLEAUX AND SYMMETRIC FUNCTIONS

The families of symmetric functions we are interested in arise as generating functions of nice families of tableaux with shape specified by a fixed partition. Therefore we will now provide a brief review of the theory of partitions and tableaux. A partition  $\lambda$  is any decreasing sequence  $\lambda = (\lambda_1, \lambda_2, \dots, \lambda_r)$  of nonnegative integers. We denote the *length* of  $\lambda$  by  $l(\lambda)$  which is the largest index  $i$  such that  $\lambda_i$  is nonzero, and the *size* of  $\lambda$  by  $|\lambda| = \lambda_1 + \lambda_2 + \dots + \lambda_r$ . A partition  $\lambda = (\lambda_1, \lambda_2, \dots, \lambda_r)$  can be visualized by its *Young diagram*, which consists of horizontal boxes arranged in left-justified rows, where the  $i^{\text{th}}$  row contains  $\lambda_i$  boxes. A *semistandard Young tableaux* of shape  $\lambda = (\lambda_1, \lambda_2, \dots, \lambda_r)$  is a labeling of the Young diagram of  $\lambda$  with elements of  $\{1, 2, \dots, r\}$  that is weakly increasing along rows and strictly increasing along columns (figure 2). Note in particular, that it is important to keep track of the number of zeros at the end of  $\lambda$ . By abuse of notation, we will not distinguish a

partition from its Young diagram. If  $\mu \subset \lambda$  for two partitions  $\lambda, \mu$ , or equivalently  $\mu_i \leq \lambda_i$  for all  $i$ , then  $\lambda/\mu$  is said to be a *skew shape* or *skew partition* with size  $|\lambda/\mu| = |\lambda| - |\mu|$ . We will identify a partition  $\lambda$  with the skew shape  $\lambda/\emptyset$ , and will also occasionally identify partitions that differ only by a sequence of zeros when it should not cause any confusion.

For the purposes of this paper, it will be most useful to think of a tableaux of skew shape  $\lambda/\mu$  as a sequence of partitions  $\mu = \lambda^0 \subset \lambda^1 \subset \dots \subset \lambda^l = \lambda$ , where  $\lambda_i$  consists of the boxes in a tableaux with labels less than or equal to  $i$  for  $i \geq 1$  (figure 2). Under this description, a semistandard Young tableau is exactly a sequence  $\mu = \lambda^0 \subset \lambda^1 \subset \dots \subset \lambda^l = \lambda$  such that for each  $i$  the skew shape  $\lambda_i/\lambda_{i-1}$  contains at most one box in each column. Such a skew shape is called a *horizontal strip*. The weight of  $T \in \text{SSYT}(\lambda/\mu)$  is then given by  $\text{wt}(T) = (|\lambda^1/\lambda^0|, |\lambda^2/\lambda^1|, \dots, |\lambda^{l-1}/\lambda^{l-2}|)$ . Visually,  $|\lambda_i/\lambda_{i-1}|$  is the number of times  $i$  appears in the tableau.

The ring of symmetric functions over  $\mathbb{Q}$  contains a distinguished basis  $\{s_\lambda\}$  indexed by partitions known as the *Schur functions*. These are given by the generating functions of semistandard Young tableaux

$$s_\lambda(X) = \sum_{T \in \text{SSYT}(\lambda)} x^{\text{wt}(T)}, \quad (4)$$

where  $\text{SSYT}(\lambda)$  denotes the set of all semistandard Young tableaux of shape  $\lambda$ , and we will write  $x = (x_1, x_2, \dots)$  and  $x^{\text{wt}(T)} = x_1^{a_1} x_2^{a_2} \dots$  when  $\text{wt}(T) = (a_1, a_2, \dots)$  for simplicity. Similarly, one can define the *skew Schur functions*  $s_{\lambda/\mu}$  as the generating functions of semistandard Young tableaux of skew shape  $\lambda/\mu$ .

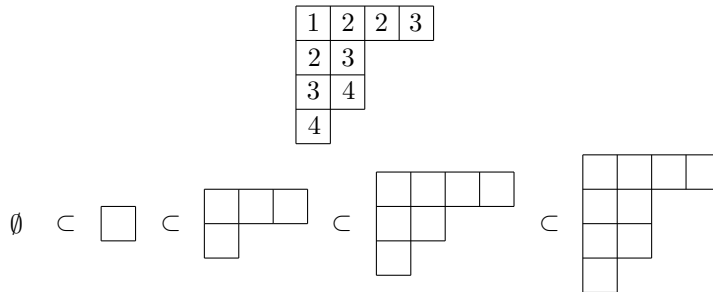
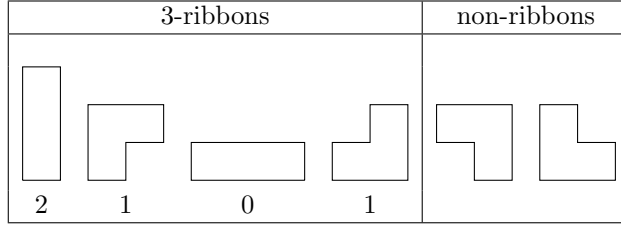


FIGURE 2. Semistandard Young Tableaux of shape  $(4,2,2,1)$  and the corresponding sequence of Young diagrams.

We now describe the fundamental objects of this paper: ribbon tableaux and LLT polynomials. We follow the notation in [Lam05b]. Let  $n$  be a fixed positive integer.

**Definition 2.1** (Ribbon). An  $n$ -*ribbon* is a skew shape  $r$  containing  $n$  boxes that is connected and contains no 2 by 2 squares. The *spin* of a ribbon  $r$  is defined to be the height of  $r$  minus one, and is denoted  $\text{spin}(r)$ .

**Example 1.** The following are all possible 3-ribbons labeled by their spin.



The last two are not 3-ribbons because they cannot be realized as skew shapes  $\lambda/\mu$ .

**Definition 2.2** (Horizontal Strip). Given a skew partition  $\lambda/\mu$ , a tiling of  $\lambda/\mu$  by  $n$ -ribbons is called a  $n$ -horizontal strip if the top-right-most square of each ribbon touches the northern boundary of  $\lambda/\mu$  (figure 3).

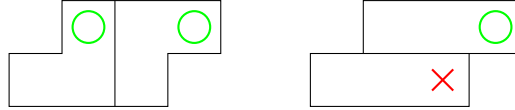


FIGURE 3. **Left:** A 3-horizontal strip. **Right:** A non-example of a horizontal strip.

**Definition 2.3.** (SSRT) We define a *semistandard  $n$ -ribbon tableaux* of skew shape  $\lambda/\mu$  to be a tiling of  $\lambda/\mu$  with  $n$ -ribbons such that the induced sequence  $\mu = \lambda^0 \subset \lambda^1 \subset \dots \subset \lambda^l = \lambda$  has the property that for each  $i$  the skew shape  $\lambda_i/\lambda_{i-1}$  is a horizontal  $n$ -ribbon strip. We define the *weight* of a semistandard  $n$ -ribbon tableaux  $T$  to be

$$\text{wt}(T) = (|\lambda^1/\lambda^0|, |\lambda^2/\lambda^1|, \dots, |\lambda^{l-1}/\lambda^l|)$$

and we define the *spin* of  $T$  to be the sum of the spins of the  $n$ -ribbon tiles of  $T$ . We denote the set of all semistandard  $n$ -ribbon tableaux by  $\text{SSRT}_n(\lambda)$ . Note that is not always possible to tile a given partition  $\lambda$  with  $n$ -ribbons, and we will restrict our attention to partitions or skew shapes that are tileable by  $n$ -ribbons.

We can now define the central object of this paper, first introduced by Lascoux, Leclerc, and Thibon in [LLT97] under the name  $n$ -ribbon Schur functions.

**Definition 2.4.** Let  $n \geq 1$  be fixed and  $\lambda/\mu$  a skew shape tileable by  $n$ -ribbons. Then the  $n$ -LLT polynomial of shape  $\lambda/\mu$  is defined as the generating function

$$\mathcal{G}_{\lambda/\mu}^{(n)}(X; q) = \sum_{T \in \text{SSRT}_n(\lambda/\mu)} q^{\text{spin}(T)} x^{\text{wt}(T)}. \tag{5}$$

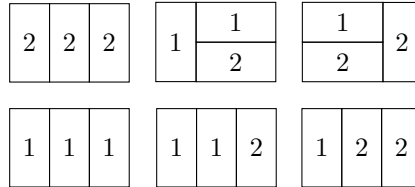


FIGURE 4. Ribbon Tableaux corresponding to  $\mathcal{G}_{(3,3)}^{(2)}$ .

For example, suppose that  $\lambda = (3, 3)$  and  $n = 2$ . It is not difficult to see that the only possible 2-ribbon tableaux are those depicted in figure 4. Now we can directly compute that

$$\mathcal{G}_{(3,3)}^{(2)}(x_1, x_2; q) = q^3(x_1^3 + x_1^2x_2 + x_1x_2^2 + x_2^3) + q(x_1^2x_2 + x_1x_2^2).$$

We will often abuse notation and write  $\mathcal{G}_{\lambda/\mu}^{(n)}(X; q) = \mathcal{G}_{\lambda/\mu}(X; q)$  when  $n$  is understood. The LLT polynomials are  $q$ -analogues of the Schur functions in the sense that  $\mathcal{G}_{\lambda/\mu}(X; 1)$  is equal to a product of  $n$  Schur functions ([LLT97]). Having defined all the relevant tableaux and symmetric functions, we now describe the lattice models of interest.

### 3. LATTICE MODELS

Exactly solvable two dimensional Ising models are of great interest in statistical mechanics, as they provide useful information about the behavior of phase transitions. The six vertex model or ice-type model from statistical mechanics is a lattice model defined on a rectangular grid. An *admissible state* for the lattice is a labeling of each edge with arrows so that at each vertex, there are two arrows pointing inward and two pointing outward. We denote a vertex by the two directions from which arrows are pointing inward, for example southwest (SW) and so on. To each vertex  $v$ , we assign a *Boltzmann weight*  $\text{wt}(v)$  taking values in  $\mathbb{Q}(x_1, x_2, \dots)$ , usually depending on which row the vertex lies in. For a given admissible state  $S$ , the weight of the lattice is defined to be the product of the Boltzmann weights at each of the vertices, that is

$$\text{wt}(S) = \prod_{v \in S} \text{wt}(v). \quad (6)$$

Given a fixed set of boundary conditions  $B$  on a rectangular grid, we define the *partition function* of a square grid to be the sum of the weights of all admissible states:

$$\mathcal{P}_B(X) = \sum_{\substack{\text{admissible states } S \text{ with} \\ \text{boundary conditions } B}} \text{wt}(S), \quad (7)$$

In this section, we describe a five vertex lattice model whose partition functions are the Schur functions, followed by a more general lattice type model that gives rise to the LLT polynomials.

#### 3.1. A Five Vertex Model for Schur Functions.

Given a fixed skew shape  $\lambda/\mu$ , where  $\lambda$  has length  $r$ , we convert  $\lambda$  from a weakly decreasing sequence to a strictly decreasing sequence by adding the vector  $\rho = (r-1, r-2, \dots, 1, 0)$ , and do the same to  $\mu$ , viewing  $\mu$  as a vector with  $r$  components by adding zeroes to the end if necessary. Now consider a square grid with  $r$  rows and  $\lambda_1 - \mu_1 + r$  columns, labeled 0 through  $\lambda_1 - \mu_1 + r - 1$ . In the top row, place an upward arrow in the columns labeled by the entries of  $\mu + \rho$ , and downward arrows for all other vertices. Similarly place upward arrows in the bottom row at every column labeled by the entries of  $\lambda + \rho$ . Finally for the left and right boundaries of the square lattice, put rightward pointing arrows at every edge. We call these boundary conditions *Schur boundary conditions of shape  $\lambda/\mu$* . We then define the *partition function*  $\mathcal{P}_{\lambda/\mu}$  of skew shape  $\lambda/\mu$  to be the partition function with respect to Schur boundary conditions of shape  $\lambda/\mu$ . When  $\mu = \emptyset$ , we often omit  $\mu$ , and just write  $\mathcal{P}_\lambda$  in place of  $\mathcal{P}_{\lambda/\mu}$ .

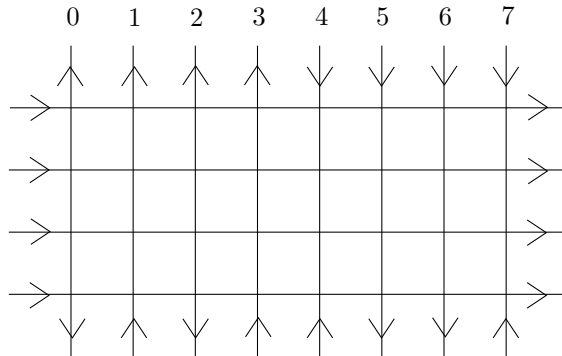


FIGURE 5. Schur boundary conditions for the six vertex model of shape  $\lambda/\mu$  with  $\lambda = (4, 2, 2, 1)$  and  $\mu = (0, 0, 0, 0)$ , so that  $\lambda + \rho = (7, 4, 3, 1)$  and  $\mu + \rho = (3, 2, 1, 0)$

Now consider the weights pictured in figure 6, noting that the weight of a vertex depends on the row it lies in. Since the SE vertex has a weight of zero, any admissible state containing a SE vertex will not contribute to the partition function. Therefore we can view this lattice as a five vertex model. Therefore, going forward, we will not consider any state with weight 0 as an admissible state. A similar five vertex model appears in [BBF09] whose partition functions are equal to  $x^p s_\lambda(x_1 x_2, \dots)$ . The advantage using the set of weights in figure 6 is that the resulting admissible states can also be interpreted as non intersecting lattice paths (NILPs) on a square grid. Furthermore, these vertex weights have a nice combinatorial interpretation that is key to understanding the connection between the five vertex model and the Schur functions.

Label	SW	NS	SE	NW	EW	NE
Vertex						
Weight	1	1	0	1	$x_i$	$x_i$

FIGURE 6. The Boltzmann weights of vertices lying in row  $i$  for the five vertex model labeled by cardinal directions.

It follows straightforwardly from the definition of Boltzmann weights that for any admissible state  $S$ ,  $\text{wt}(S) = \prod_{i=1}^r x_i^{a_i}$ , where  $a_i$  is the number of leftward pointing arrows in row  $i$ . This observation motivates the following result.

**Theorem 3.1.** *There is a weight preserving bijection  $\Phi$  from the set  $\text{SSYT}(\lambda/\mu)$  to the set of admissible lattice states with Schur boundary conditions of shape  $\lambda/\mu$  such that  $\text{wt}(\Phi(T)) = x^{\text{wt}(T)}$  for  $T \in \text{SSYT}(\lambda/\mu)$ .*

*Proof.* Consider some semistandard Young tableaux  $T = (\mu = \lambda^0 \subset \lambda^1 \subset \dots \subset \lambda^l = \lambda)$ . By adding zeros if necessary, assume each  $\lambda_i$  has length  $l(\lambda) = r$ . Now define  $\gamma_i = \lambda_i + \rho$ , where  $\rho = (r - 1, r - 2, \dots, 0)$ .

1	2	2	3
2	3		
3	4		
4			

FIGURE 7. Semistandard Young tableaux of the partition  $(4, 2, 2, 1)$ .

Given a grid with Schur boundary conditions of shape  $\lambda/\mu$  with  $\lambda_1 - \mu_1 + r$  columns and  $r$  rows, assign the interior vertical arrows according to the following rule: for a fixed  $i$  in  $2, 3, \dots, r$  the vertical arrows directly above row  $i$  and in column  $j$  are pointing upward if  $j$  is an entry of  $\gamma_{i-1}$ , and are pointing downwards otherwise (recall that we are labeling the columns starting at 0 and ending at  $\lambda_1 - \mu_1 + r - 1$ ).

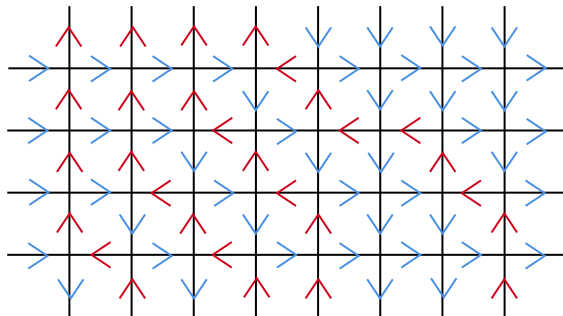


FIGURE 8. Lattice model associated to the semistandard Young tableaux in Figure 7.

Since no admissible state contains a SE vertex, it is easy to see that the assignment of vertical arrows will determine a unique assignment of horizontal arrows corresponding naturally to a NILP. Now that the bijection is weight-preserving follows from the bijection between semistandard Young tableaux and NILP's described in [Sta99b] Section 7.16.  $\square$

*Remark 3.1.* For a SSYT  $T = (\mu = \lambda^0 \subset \lambda^1 \subset \dots \subset \lambda^l = \lambda)$  and its corresponding lattice model, we notice that the vertical arrows in each row match the edge sequences of the partitions  $\lambda^0, \dots, \lambda^l$ , see figure 9 for an example. This provides an alternative way to describe the bijection.

We obtain the following as an immediate corollary.

**Corollary 3.2.** *For any skew shape  $\lambda/\mu$ , the partition function  $\mathcal{P}_{\lambda/\mu}(x_1, \dots, x_r)$  is equal to the skew Schur function  $s_{\lambda/\mu}(x_1, \dots, x_r)$ .*

In view of the previous corollary, many nice identities of Schur functions can be proved using properties of lattice models. For example, consider some admissible lattice state  $S$  with Schur boundary conditions of shape  $\lambda$ . Below the  $r^{\text{th}}$  row, there are vertical arrows positioned according to the entries of  $\lambda + \rho$ . Directly above the

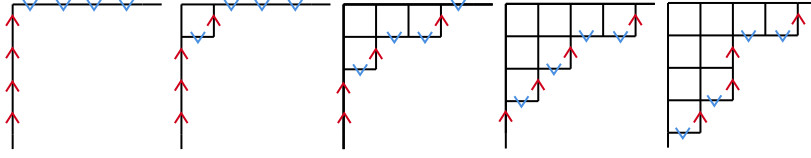


FIGURE 9. The edge sequences of the sequence of partitions defining the SSYT in figure 7. Viewing the vertical edges as up arrows and horizontal edges as down arrows, these edge sequences match exactly the vertical arrows in each row of figure 8.

$r^{\text{th}}$  row, there are vertical arrows positioned according to  $\gamma + \rho$ , where  $\lambda/\gamma$  is a horizontal strip, which we will denote by  $\gamma \prec \lambda$ . For a fixed  $\gamma \prec \lambda$ , exactly  $|\lambda/\gamma|$  vertices in the  $r^{\text{th}}$  row will have weight  $x_r$ , and all the remaining vertices in that row will have weight 1. It readily follows that

**Proposition 3.3.** *If  $\lambda/\mu$  is a skew shape, then*

$$s_{\lambda/\mu}(x_1, \dots, x_r) = \sum_{\gamma \prec \lambda} x_r^{|\lambda/\gamma|} s_{\gamma/\mu}(x_1, \dots, x_{r-1}). \quad (8)$$

Splitting the lattice diagram at any row instead of the bottom row gives rise to more general branching identities:

**Proposition 3.4.** *Let  $\lambda/\mu$  be a skew shape of length  $r$  and  $\gamma \subset \lambda$  a fixed partition such that  $\lambda/\gamma$  has length  $k$ . Then*

$$s_{\lambda/\mu}(x_1, \dots, x_r) = \sum_{T \in \text{SSYT}(\lambda/\gamma, k)} x_{-(k+1)}^{\text{wt}(T)} s_{\gamma/\mu}(x_1, \dots, x_k), \quad (9)$$

$$s_{\lambda/\mu}(x_1, \dots, x_r) = \sum_{T \in \text{SSYT}(\gamma/\mu, k)} x^{\text{wt}(T)} s_{\lambda/\gamma}(x_{r-k+1}, \dots, x_r), \quad (10)$$

where we denote  $x_{-(k+1)}^{\text{wt}(T)} = x_{k+1}^{a_1} \cdots x_r^{a_k}$  whenever  $\text{wt}(T) = (a_1, \dots, a_k)$ , and  $\text{SSYT}(\lambda/\gamma, k)$  is the set of semistandard Young tableaux of skew shape  $\lambda/\gamma$  with labels in  $\{1, \dots, k\}$ .

### 3.2. Ribbon Lattice Models.

Throughout this section, fix some  $n \geq 1$ . We now describe an extension of the 5 vertex model that is connected to  $n$ -th LLT polynomials, which we call the  $n$ -ribbon lattice model. Similar to the ice-type models, the vertices in ribbon lattice models also take place in some rectangular lattice  $[a] \times [b]$ , where  $[n] = \{1, \dots, n\}$ . We denote the north, south, east and west entries of a vertex  $v$  by  $v_N, v_S, v_W$  and  $v_E$  respectively.

The horizontal entries of a vertex  $v_W = (v_W(1), \dots, v_W(n))$  and  $v_E = (v_E(1), \dots, v_E(n))$  are  $n$ -tuples of either left or right arrows, and the vertical entries  $v_N$  and  $v_S$  are simply up or down arrows as usual (figure 10). We think of these decorations as arrows pointing either in or out of the vertex  $v$ .

Before defining the weight of a vertex, there are a few conditions that are necessary for a vertex  $v$  to be admissible.

**Definition 3.1** (admissible vertices). A  $n$ -ribbon vertex  $v$  is said to be *admissible* if it satisfies the following conditions.

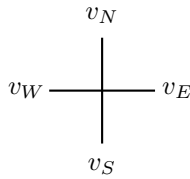


FIGURE 10. A vertex of a  $n$ -ribbon lattice, where  $v_W = (v_W(1), \dots, v_W(n))$  and  $v_E = (v_E(1) \dots v_E(n))$  and  $v_N, v_S, v_E(i), v_W(i) \in \{+, -\}$

- (1) The number of arrows pointing inwards equals the number of arrows pointing outwards.
- (2) We require that  $v_E(i) = v_W(i + 1)$  for all  $i \in \{1, 2, \dots, n - 1\}$ . Note that  $v_E(n)$  need not be equal to  $v_W(1)$ .
- (3) The vertex  $v$  with  $v_N = v_S = \text{up}$  and  $v_W(1) = v_E(n) = \text{left}$  is not admissible.

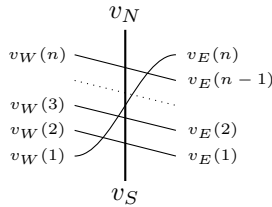


FIGURE 11. A  $n$ -ribbon vertex.

In light of condition (2), we draw lines between  $v_E(i)$  and  $v_W(i + 1)$  for  $i = 1, 2, \dots, n - 1$  in addition to a line between  $v_E(1)$  and  $v_W(n)$  as in figure 11<sup>1</sup>. Figure 12 is the drawing of a entire square lattice with intertwining horizontal edges.

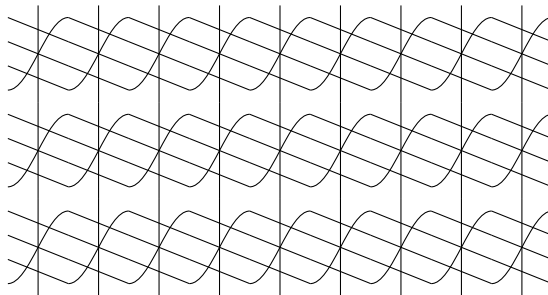


FIGURE 12. A 4-ribbon lattice with arrows omitted.

We will call the edge from  $v_W(1)$  to  $v_E(n)$  the *twisted edge*, and every other horizontal edge will be called *straight*. Then we can summarize the second condition

<sup>1</sup>From now on, we will present the vertices as figure 11, although they don't look like *vertices* anymore.

concisely by requiring that arrows do not change along any straight edge. Therefore every left arrow occurring at  $v_E(n)$  must be following by  $n - 1$  consecutive left arrows from the right along its strand (figure 13).

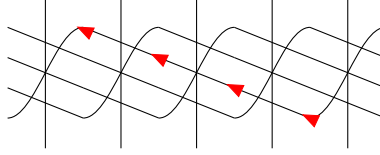


FIGURE 13. The  $v_E(4)$  entry of the leftmost vertex is a left arrow, which must be following by 3 left arrows from the right.

**Definition 3.2** (*n*-ribbon lattice models). We define a *n*-ribbon lattice to be a rectangular grid of admissible vertices  $v[i, j]$  where  $1 \leq i \leq a$  and  $1 \leq j \leq b$  for fixed positive integers  $a, b$  such that the left vertices of one vertex  $v$  agree with the right vertices of the vertex  $w$  located to the left of  $v$ , and so on. Notice that when  $n = 1$  this is just the 5 vertex model described earlier. In general, there are  $2^{n-1}$  choices for the vertices  $v_R(1), v_E(2), \dots, v_E(n - 1)$ , and these uniquely determine the edge values  $v_L(2), v_E(3), \dots, v_W(n)$ . Then we just need to choose values for  $v_N, v_S, v_W(1)$ , and  $v_E(n)$ , and it is easy to see that there are exactly 5 choices for an admissible vertex, so there are a total of  $5 \cdot 2^{n-1}$  admissible vertices.

We now define the Boltzmann weights for the admissible vertices which, unlike the 5-vertex model, live in  $\mathbb{Q}(q, x_1, x_2, \dots)$ .

**Definition 3.3** (Boltzmann weights). Any vertex that is not admissible will be given a weight of 0. Given any admissible vertex  $v$  in the  $i$ -th row, we define its weight by

$$\text{wt}(v) = x_i^{\varepsilon(v)} \cdot q^{\sigma(v)}, \tag{11}$$

where

$$\varepsilon(v) = \begin{cases} 1 & \text{if } v_E(n) = \text{left} \\ 0 & \text{otherwise;} \end{cases} \tag{12}$$

$$\sigma(v) = \begin{cases} L(v) & \text{if } v_N = v_S = \text{up}, v_W(1) = v_E(n) = \text{right (SW)} \\ L(v) & \text{if } v_N = \text{down}, v_S = \text{up (NS)} \\ L(v) - 1 & \text{if } v_N = \text{up}, v_S = \text{down (EW)} \\ L(v) - 1 & \text{if } v_N = v_S = \text{down}, v_W(1) = v_E(n) = \text{left (NE)} \\ 0 & \text{otherwise.} \end{cases} \tag{13}$$

where  $L(v)$  is the number of left arrows in  $v_E$ . These weights can be described pictorially in figure 14, where the spin weight has a nice interpretation: the exponent  $\sigma(v)$  of  $q$  is exactly the number of left arrows in each blue circled area.

Label	SW	NS	SE	NW	EW	NE
Vertex						
Weight	$q^s$	$q^s$	0	1	$q^s x_i$	$q^s x_i$

FIGURE 14. The weights of vertices lying in row  $i$  for the  $n$ -ribbon lattice model, where  $s$  is the number of left arrows in the blue circled area. Note that vertices of type SE is not admissible.

**Definition 3.4** (Boundary conditions). The boundary conditions of the  $n$ -ribbon lattice models are very similar to the boundary conditions for the 5-vertex models (the case of  $n = 1$ ). For a skew shape  $\lambda/\mu$ , the top and lower boundaries of the rectangular grid are defined exactly as before by adding  $\rho$  to  $\lambda$  and  $\mu$  and using the shifted entries to determine where to place the up arrows. Along the left and right boundary, we force that all the outer arrows point right, that is,  $v[1, i]_L$  and  $v[a, i]_R$  consist of only right arrows for all  $i$ . We call these boundary conditions  *$n$ -ribbon boundary conditions*, and denote them by  $\mathcal{B}_{\lambda/\mu}$ .

Now we can provide an alternative way of modeling the LLT polynomials.

**Theorem 3.5.** Let  $\mathcal{R}_{\lambda/\mu}^{(n)}(X; q)$  be the partition function of the  $n$ -ribbon lattice model with boundary condition  $\mathcal{B}_{\lambda/\mu}$ . We have

$$\mathcal{R}_{\lambda/\mu}^{(n)}(X; q) = \mathcal{G}_{\lambda/\mu}^{(n)}(X; q)$$

The structure of the ribbon lattice gives rise to combinatorial proofs of LLT polynomial identities. For example, splitting along any row and computing the partition function of a grid in two different ways, we obtain an analogue of proposition 3.4:

**Proposition 3.6** (Branching Rule).

$$\mathcal{G}_{\lambda/\mu}^{(n)}(x_1, \dots, x_r; q) = \sum_{T \in \text{SSRT}_n(\lambda/\gamma, k)} q^{\text{spin}(T)} x_{-(k+1)}^{\text{wt}(T)} \mathcal{G}_{\gamma/\mu}^{(n)}(x_1, \dots, x_k; q), \quad (14)$$

$$\mathcal{G}_{\lambda/\mu}^{(n)}(x_1, \dots, x_r; q) = \sum_{T \in \text{SSRT}_n(\gamma/\mu, k)} q^{\text{spin}(T)} x_{r-k+1}^{\text{wt}(T)} \mathcal{G}_{\lambda/\gamma}^{(n)}(x_{r-k+1}, \dots, x_r; q), \quad (15)$$

where we write  $x_{-(k+1)}^{\text{wt}(T)} = x_{k+1}^{a_1} \cdots x_r^{a_k}$  whenever  $\text{wt}(T) = (a_1, \dots, a_k)$ , and  $\text{SSRT}_n(\lambda/\gamma, k)$  is the set of semistandard  $n$ -ribbon tableaux of skew shape  $\lambda/\gamma$  with labels in  $[k]$ .

#### 4. PROOF OF THEOREM 3.5

In this section, we prove theorem 3.5 by constructing a weight preserving bijection between the set of all ribbon tableaux and the set of all admissible ribbon lattices with the corresponding boundary conditions. We start with an important lemma.

**Lemma 4.1.** Consider an one-row ribbon lattice model with boundary given by  $\mathcal{B}_{\lambda/\mu}$ . If  $\lambda/\mu$  is a horizontal  $n$ -ribbon strip, then there is a unique admissible state. Otherwise, there are no admissible states with boundary  $\mathcal{B}_{\lambda/\mu}$ .

*Proof.* The condition  $v_E(i) = v_W(i + 1)$  implies that any admissible state can be broken up into  $n$  different admissible states of the 1-ribbon lattice where each vertex only interacts with vertices a multiple of  $n$  away from them. Theorem 3.1 then implies there is at most one admissible lattice state for  $\lambda/\mu$ .

We create a map from a set of  $n$ -ribbons which form a horizontal  $n$ -ribbon strip in  $\lambda/\mu$  to an admissible state with boundary  $\mathcal{B}$ . By considering the effect of “peeling off” successive ribbon strips from  $\lambda$ , we create a sequence of admissible states which we then merge into a single lattice row. We start at the rightmost ribbon  $r_1$  and create an admissible state for  $\lambda/(\lambda \setminus r_1)$ .

To the rightmost vertex  $v$ , we assign a down arrow to the north edge and an up arrow to the south edge. We then add a left arrow at  $v_W(1)$  and use the rule  $v_E(i) = v_W(i + 1)$  to add left arrows to  $n - 1$  of  $v$ 's leftward neighbors. Filling out the remainder of the lattice with right arrows gives an admissible lattice state for  $\lambda/(\lambda \setminus r_1)$ . Then we apply the above process to  $(\lambda \setminus r_1)/(\lambda \setminus r_1 \cup r_2)$  where  $r_2$  is the rightmost ribbon in  $(\lambda \setminus r_1)$ , and so forth. When we finish we will have a set of admissible lattices for  $(\lambda \setminus \bigcup_{i=1}^k r_i)/(\lambda \setminus \bigcup_{i=1}^{k+1} r_i)$ , one for each  $k$  from 0 to the number of ribbons.

Now we construct the admissible lattice state for  $\lambda/\mu$  by filling in the interior with the union of the sets of left arrows in each of the above lattice states. There are four things to check to make sure this is an admissible lattice state:

- (1) For every vertex  $v$ ,  $v_E(i) = v_W(i + 1)$ ,
- (2) every vertex has an equal number of in and out arrows,
- (3) there are no vertices of type SE.

Since each ribbon has an upper right corner which borders the top of the horizontal  $n$ -ribbon strip, we know that  $\lambda \setminus \bigcup_{i=1}^k r_k$  must agree with  $\mu$  everywhere to the right of and including the rightmost vertex of  $r_k$ . It follows that if  $v_W(1)$  points left, there is no up arrow above  $v$ , proving (3). For (2),  $v_E(i) = v_W(i + 1)$  and the above statement shows that all sets of left arrows in  $(\lambda \setminus \bigcup_{i=1}^k r_i)/(\lambda \setminus \bigcup_{i=1}^{k+1} r_i)$  are distinct from those in  $(\lambda \setminus \bigcup_{i=1}^s r_i)/(\lambda \setminus \bigcup_{i=1}^{s+1} r_i)$  for  $s \neq k$ ; (2) then follows from each of  $(\lambda \setminus \bigcup_{i=1}^k r_i)/(\lambda \setminus \bigcup_{i=1}^{k+1} r_i)$  being an admissible lattice state. (1) follows from all the sets of left arrows we are unioning including  $v_E(i) = v_W(i + 1)$ . Moreover, this also implies that filling out the edges does not violate the boundary condition  $\mathcal{B}$ .

We can reverse the above process, starting from the leftmost side of an admissible state and constructing ribbons in  $\lambda/\mu$  whose union forms a horizontal  $n$ -ribbon. This implies the second statement of our proposition.  $\square$

Theorem 3.5 is an immediate corollary of the following result.

**Theorem 4.2.** *There exists a weight preserving bijection between admissible states of an  $n$ -ribbon lattice model with  $n$ -ribbon boundary conditions of shape  $\lambda/\mu$  and semistandard  $n$ -ribbon tableaux of shape  $\lambda/\mu$ .*

We prove theorem 4.2 in two steps. First we will define the bijection, and then we provide a graphical description of this bijection. From this interpretation, it will become obvious that the bijection is weight-preserving.

To define the bijection, we view a ribbon tableaux as a sequence of partitions  $\mu = \lambda^1 \subset \lambda^1 \subset \dots \subset \lambda^r = \lambda$ . We assign the vertical arrows in the same manner as in theorem 3.1. By lemma 4.1, this map is a bijection. This bijection can be understood visually. The ribbon lattices have the graphical interpretation that when moving from one row to the row above it, the up arrows are allowed to

travel to the left in steps of size divisible by  $n$  as we view the left arrows as their ‘footprints’, where the weight picks up a factor of  $x_i$  each time an up arrow moves to the left for  $n$  steps and a factor of  $q$  each time when a moving arrows meets another up-arrow. The paths of the movements of up-arrows can be seen from the tableaux concretely with the help of the *edge sequence* of a partition.

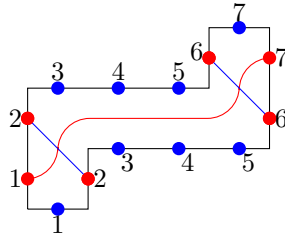


FIGURE 15. The edge sequence path of a 6-ribbon

Consider a single ribbon, we label each vertical (resp. horizontal) edge red (resp. blue) and number their positions increasingly from left to right. Under the bijection, the red (resp. blue) edges correspond to the up (resp. down) arrows in the lattice. Along each  $n$ -ribbon, the red dot in the upper right corner will travel to the lower left corner, and all the remaining reds will travel up and to the left while position remains (figure 15). We call this the *edge sequence path* of a ribbon. Notice that the definition of horizontal ribbon strip guarantees this construction. In another word, ribbons that are not compatible with an edge sequence path must fail the requirement of being a horizontal strip.

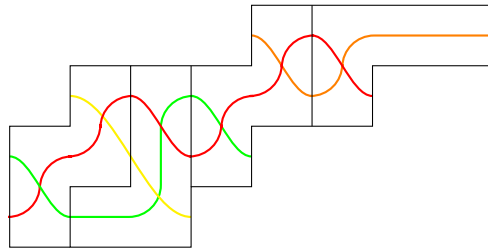


FIGURE 16. The edge sequence path of a horizontal strip

In an  $n$ -ribbon horizontal strip, since the top right edge of each constituent  $n$ -ribbon lies on the upper edge of the skew shape the paths just described can simply be glued together, we can define the edge sequence path for a ribbon tableau by gluing up the same construction on each pieces of ribbons. These paths are identical to the movement of up-arrows in a ribbon lattice. For example, the one-row lattice model which corresponds to figure 16 is drawn in figure 17, where the arrows are colored in a specific way that indicates the movement of each arrow, which exactly matches the colors of their corresponding edge sequence paths in figure 16.

*Proof of Theorem 4.2.* Now that the map is weight preserving follows naturally from the path interpretation of the ribbon lattices. In a fixed row  $i$ , the weight is

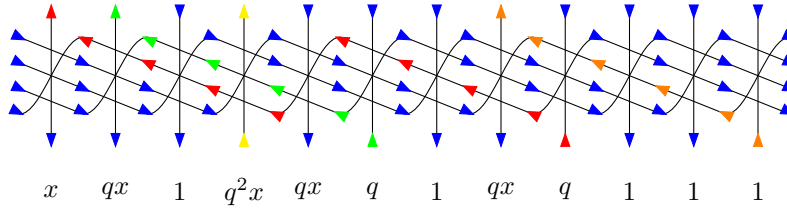


FIGURE 17. Single row lattice of the horizontal strip in Figure 16, with colors indicating movements of up-arrows. One can verify that the partition function is  $q^7 x_i^4$ .

given by a power of  $q$  times the  $x_i^a$  where  $a$  is the number of times an arrow moves  $n$  steps to the left. This corresponds exactly to the number of ribbons because within each ribbon, there is one up-arrow moved  $n$  steps leftwards and all other up-arrows remains (figure 15). On the other hand, the power of  $q$  counts the number of intersection of the paths, which is exactly the value of the spin.  $\square$

5. EXACT SOLVABILITY

Lattice models satisfying a Yang-Baxter equation are called *exactly solvable*, or *integrable*. From the lattice model perspective, the Yang Baxter equation gives a consistent way of effectively permuting the weights of an admissible state without altering the partition function. In particular, it implies that the partition functions are in fact symmetric functions.

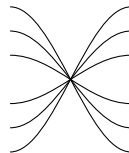


FIGURE 18. ‘New’ vertex for the Yang-Baxter Equation of a 3-ribbon lattice.

The Yang-Baxter Equation for a  $n$ -ribbon lattice model is asking for a proper choice Boltzmann weights for a set of new vertices of in-degree  $2n$  and out-degree  $2n$  (e.g. figure 18), such that the partition functions (equation (16)) of the two ‘mini’ lattice models are equal for any fixed boundary conditions. A complete treatment of Yang-Baxter equations of  $2-d$  square lattice models is referred to [BBF09, section 1& 5] and [Bax89, chapter 8& 9].

$$\mathcal{P}_B \left( \begin{array}{c} \text{Diagram 1} \\ \text{Diagram 2} \\ \text{Diagram 3} \\ \text{Diagram 4} \\ \text{Diagram 5} \\ \text{Diagram 6} \\ \text{Diagram 7} \\ \text{Diagram 8} \end{array} \right) = \mathcal{P}_B \left( \begin{array}{c} \text{Diagram 1} \\ \text{Diagram 2} \\ \text{Diagram 3} \\ \text{Diagram 4} \\ \text{Diagram 5} \\ \text{Diagram 6} \\ \text{Diagram 7} \\ \text{Diagram 8} \end{array} \right) \tag{16}$$

By direct computation, we obtain solutions for the Yang Baxter equation for 1,2 and 3 ribbon lattices. The YBE for  $n = 1$  is given as follows.

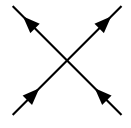
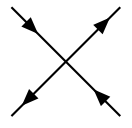
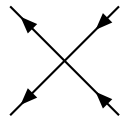
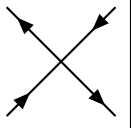
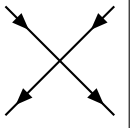
Vertex						
Weight	0	1	1	$z_i$	$z_i$	$z_i - 1$

FIGURE 19. Solution to YBE for the 1-ribbon lattice model, where  $z_i = x_i/x_{i+1}$

We will show the solutions to the Yang-Baxter Equations for 2,3-ribbon lattice models in section A. For  $n \geq 4$ , solving the Yang-Baxter equation is too computationally complex to be calculated in a reasonable amount of time. We conjecture that the ribbon lattices are exactly solvable for all  $n$ , that a proof for all  $n$  would likely involve a deep connection between the lattice model and the quantum affine algebra  $U_q(\widehat{\mathfrak{sl}}_n)$ .

## 6. FUTURE DIRECTIONS

The methods in this paper are quite different from the previous methods to study LLT polynomials, which generally rely on the action of a Heisenberg algebra of the Fock space of the quantum affine algebra  $U_q(\widehat{\mathfrak{sl}}_n)$ . Lattice models are useful tool for studying symmetric polynomials and giving combinatorial proofs of interesting identities, for example [BBF09, BMN11]. There are identities that are known for Schur functions that are not known for LLT polynomials that can be proved using the bijection between semistandard Young tableaux and the five vertex model. For example, there is no analog of the Jacobi-Trudi identity for Schur functions that is known to hold for arbitrary  $n$ -LLT polynomials. There is, however, a proof of the Jacobi-Trudi identity in [Sta99a, Sta99b] using the bijection in theorem 3.1, and it would be worthwhile to investigate if a similar identity can be derived from ribbon lattice models.

## REFERENCES

- [Bax89] Rodney Baxter. *Exactly Solved Models in Statistical Mechanics*. Academic Press Limited, 1989.
- [BBF09] Ben Brubaker, Daniel Bump, and Solomon Friedberg. Schur Polynomials and the Yang-Baxter equation. *arXiv e-prints*, page arXiv:0912.0911, Dec 2009.
- [BMN11] Daniel Bump, Peter J McNamara, and Maki Nakasuji. Factorial schur functions and the yang-baxter equation. *arXiv preprint arXiv:1108.3087*, 2011.
- [Lam05a] Thomas Lam. A combinatorial generalization of the Boson-Fermion correspondence. *arXiv Mathematics e-prints*, page math/0507341, Jul 2005.
- [Lam05b] Thomas Lam. Ribbon tableaux and the heisenberg algebra. *Mathematische Zeitschrift*, 250(3):685–710, 2005.
- [LLT97] Alain Lascoux, Bernard Leclerc, and Jean-Yves Thibon. Ribbon tableaux, hall–littlewood functions, quantum affine algebras, and unipotent varieties. *Journal of Mathematical Physics*, 38(2):1041–1068, 1997.
- [Sta99a] Richard Stanley. *Enumerative Combinatorics, Volume 1*. Cambridge University Press, 1999.

- [Sta99b] Richard Stanley. *Enumerative Combinatorics, Volume 2*. Cambridge University Press, 1999.
- [ZJ09] Paul Zinn-Justin. Six-vertex, loop and tiling models: integrability and combinatorics. *arXiv preprint arXiv:0901.0665*, 2009.

A. YANG-BAXTER EQUATION FOR 2, 3-RIBBON LATTICE MODELS

In this appendix, we demonstrate the solutions to the Yang-Baxter equations for 2 and 3-ribbon lattice models.

A.1.  $n = 2$  **case.** Solutions to the YBE of 2-ribbon lattice model are weights associated to the vertex in figure 20, whose edges are decorated by left (+) or right (-) arrows.

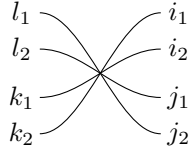


FIGURE 20. Solution to the Yang-Baxter Equation of a 2-ribbon lattice.

Labeling the edges by  $i_1, i_2, j_1, j_2, k_1, k_2, l_1, l_2$  as shown in figure 20, the non-zero Boltzmann weights are given in the following table.

Table 1:  $n = 2$  Yang-Baxter Equation

$i_1$	$i_2$	$j_1$	$j_2$	$k_1$	$k_2$	$l_1$	$l_2$	weight
-	-	-	-	-	-	-	-	$x_0/x_1$
-	-	+	-	+	-	-	-	1
-	-	-	+	-	+	-	-	1
-	-	+	+	+	+	-	-	$x_1/x_0$
+	-	-	-	-	-	+	-	$x_0/x_1$
+	-	-	-	+	-	-	-	$(x_0 - x_1)/x_1$
+	-	+	-	+	-	+	-	1
+	-	-	+	-	+	+	-	1
+	-	-	+	+	+	-	-	$(x_0 - x_1)/x_0$
+	-	+	+	+	+	+	-	$x_1/x_0$
-	+	-	-	-	-	-	+	$x_0/x_1$
-	+	-	-	-	+	-	-	$(x_0 - x_1)/x_1$
-	+	+	-	+	-	-	+	1
-	+	+	-	+	+	-	-	$(x_0 - x_1)/(qx_0)$
-	+	-	+	-	+	-	+	1
-	+	+	+	+	+	-	+	$x_1/x_0$
+	+	-	-	-	-	+	+	$x_0/x_1$
+	+	-	-	+	-	-	+	$(x_0 - x_1)/(qx_1)$
+	+	-	-	-	+	+	-	$(x_0 - x_1)/x_1$
+	+	-	-	+	+	-	-	$(q^2x_0 - x_1)(x_0 - x_1)/(q^2x_0x_1)$
+	+	+	-	+	-	+	+	1
+	+	+	-	+	+	+	-	$(x_0 - x_1)/(qx_0)$

Continuation of Table 1								
$i_1$	$i_2$	$j_1$	$j_2$	$k_1$	$k_2$	$l_1$	$l_2$	weight
+	+	-	+	-	+	+	+	1
+	+	-	+	+	+	-	+	$(x_0 - x_1)/(qx_0)$
+	+	+	+	+	+	+	+	$x_1/x_0$
End of Table								

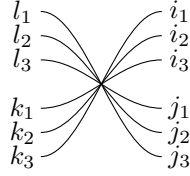


FIGURE 21. Solution to the Yang-Baxter Equation of a 3-ribbon lattice.

A.2.  $n = 3$  case. We labeling the edges in figure 21 in a similar way. The configurations with non-zero Boltzmann weights are given in the following table.

Table 2:  $n = 3$  Yang-Baxter Equation

$i_1$	$i_2$	$i_3$	$j_1$	$j_2$	$j_3$	$k_1$	$k_2$	$k_3$	$l_1$	$l_2$	$l_3$	weight
-	-	-	-	-	-	-	-	-	-	-	-	1
-	-	-	+	-	-	+	-	-	-	-	-	$x_1/x_0$
-	-	-	-	+	-	-	+	-	-	-	-	$x_1/x_0$
-	-	-	-	-	+	-	-	+	-	-	-	$x_1/x_0$
-	-	-	+	+	-	+	+	-	-	-	-	$x_1^2/x_0^2$
-	-	-	+	-	+	+	-	+	-	-	-	$x_1^2/x_0^2$
-	-	-	-	+	+	-	+	+	-	-	-	$x_1^2/x_0^2$
-	-	-	+	+	+	+	+	+	-	-	-	$x_1^3/x_0^3$
+	-	-	-	-	-	-	-	-	+	-	-	1
+	-	-	-	-	-	+	-	-	-	-	-	$(x_0 - x_1)/x_0$
+	-	-	+	-	-	+	-	-	+	-	-	$x_1/x_0$
+	-	-	-	+	-	-	+	-	+	-	-	$x_1/x_0$
+	-	-	-	+	-	+	+	-	-	-	-	$(x_0 - x_1)x_1/x_0^2$
+	-	-	-	-	+	-	-	+	+	-	-	$x_1/x_0$
+	-	-	-	-	+	+	-	+	-	-	-	$(x_0 - x_1)x_1/x_0^2$
+	-	-	+	+	-	+	+	-	+	-	-	$x_1^2/x_0^2$
+	-	-	+	-	+	+	-	+	+	-	-	$x_1^2/x_0^2$
+	-	-	-	+	+	-	+	+	+	-	-	$x_1^2/x_0^2$
+	-	-	-	+	+	+	+	+	-	-	-	$(x_0 - x_1)x_1^2/x_0^3$
+	-	-	+	+	+	+	+	+	+	-	-	$x_1^3/x_0^3$
-	+	-	-	-	-	-	-	-	-	+	-	1
-	+	-	-	-	-	-	+	-	-	-	-	$(x_0 - x_1)/x_0$
-	+	-	+	-	-	+	-	-	-	+	-	$x_1/x_0$
-	+	-	+	-	-	+	+	-	-	-	-	$(x_0 - x_1)x_1/(qx_0^2)$
-	+	-	-	+	-	-	+	-	-	+	-	$x_1/x_0$

Continuation of Table 2												
$i_1$	$i_2$	$i_3$	$j_1$	$j_2$	$j_3$	$k_1$	$k_2$	$k_3$	$l_1$	$l_2$	$l_3$	weight
-	+	-	-	-	+	-	-	+	-	+	-	$x_1/x_0$
-	+	-	-	-	+	-	+	+	-	-	-	$(x_0 - x_1)x_1/x_0^2$
-	+	-	+	+	-	+	+	-	-	+	-	$x_1^2/x_0^2$
-	+	-	+	-	+	+	-	+	-	+	-	$x_1^2/x_0^2$
-	+	-	+	-	+	+	+	+	-	-	-	$(x_0 - x_1)x_1^2/(qx_0^3)$
-	+	-	-	+	+	-	+	+	-	+	-	$x_1^2/x_0^2$
-	+	-	+	+	+	+	+	+	-	+	-	$x_1^3/x_0^3$
-	-	+	-	-	-	-	-	-	-	-	+	1
-	-	+	-	-	-	-	-	+	-	-	-	$(x_0 - x_1)/x_0$
-	-	+	+	-	-	+	-	-	-	-	+	$x_1/x_0$
-	-	+	+	-	-	+	-	+	-	-	-	$(x_0 - x_1)x_1/(qx_0^2)$
-	-	+	-	+	-	-	+	-	-	-	+	$x_1/x_0$
-	-	+	-	+	-	-	+	+	-	-	-	$(x_0 - x_1)x_1/(qx_0^2)$
-	-	+	-	-	+	-	-	+	-	-	+	$x_1/x_0$
-	-	+	+	+	-	+	+	-	-	-	+	$x_1^2/x_0^2$
-	-	+	+	+	-	+	+	+	-	-	-	$(x_0 - x_1)x_1^2/(q^2x_0^3)$
-	-	+	+	-	+	+	-	+	-	-	+	$x_1^2/x_0^2$
-	-	+	-	+	+	-	+	+	-	-	+	$x_1^2/x_0^2$
-	-	+	+	+	+	+	+	+	-	-	+	$x_1^3/x_0^3$
+	+	-	-	-	-	-	-	-	-	+	+	1
+	+	-	-	-	-	+	-	-	-	+	-	$(x_0 - x_1)/(qx_0)$
+	+	-	-	-	-	-	+	-	+	-	-	$(x_0 - x_1)/x_0$
+	+	-	-	-	-	+	+	-	-	-	-	$(q^2x_0 - x_1)(x_0 - x_1)/(q^2x_0^2)$
+	+	-	+	-	-	+	-	-	+	+	-	$x_1/x_0$
+	+	-	+	-	-	+	+	-	+	-	-	$(x_0 - x_1)x_1/(qx_0^2)$
+	+	-	-	+	-	-	+	-	+	+	-	$x_1/x_0$
+	+	-	-	+	-	+	+	-	-	+	-	$(x_0 - x_1)x_1/(qx_0^2)$
+	+	-	-	-	+	-	-	+	+	+	-	$x_1/x_0$
+	+	-	-	-	+	+	-	+	-	+	-	$(x_0 - x_1)x_1/(qx_0^2)$
+	+	-	-	-	+	-	+	+	+	-	-	$(x_0 - x_1)x_1/x_0^2$
+	+	-	-	-	+	+	+	+	-	-	-	$(q^2x_0 - x_1)(x_0 - x_1)x_1/(q^2x_0^3)$
+	+	-	+	+	-	+	+	-	+	+	-	$x_1^2/x_0^2$
+	+	-	+	-	+	+	-	+	+	+	-	$x_1^2/x_0^2$
+	+	-	+	-	+	+	+	+	+	-	-	$(x_0 - x_1)x_1^2/(qx_0^3)$
+	+	-	-	+	+	-	+	+	+	+	-	$x_1^2/x_0^2$
+	+	-	-	+	+	+	+	+	-	+	-	$(x_0 - x_1)x_1^2/(qx_0^3)$
+	+	-	+	+	+	+	+	+	+	+	-	$x_1^3/x_0^3$
+	-	+	-	-	-	-	-	-	-	+	-	1
+	-	+	-	-	-	+	-	-	-	-	+	$(x_0 - x_1)/(qx_0)$
+	-	+	-	-	-	-	-	+	+	-	-	$(x_0 - x_1)/x_0$
+	-	+	-	-	-	+	-	+	-	-	-	$(q^2x_0 - x_1)(x_0 - x_1)/(q^2x_0^2)$
+	-	+	+	-	-	+	-	-	+	-	+	$x_1/x_0$
+	-	+	+	-	-	+	-	+	+	-	-	$(x_0 - x_1)x_1/(qx_0^2)$
+	-	+	-	+	-	-	+	-	+	-	+	$x_1/x_0$
+	-	+	-	+	-	+	+	-	-	-	+	$(x_0 - x_1)x_1/(qx_0^2)$

Continuation of Table 2												
$i_1$	$i_2$	$i_3$	$j_1$	$j_2$	$j_3$	$k_1$	$k_2$	$k_3$	$l_1$	$l_2$	$l_3$	weight
+	-	+	-	+	-	-	+	+	+	-	-	$(x_0 - x_1)x_1/(qx_0^2)$
+	-	+	-	+	-	+	+	+	-	-	-	$(q^2x_0 - x_1)(x_0 - x_1)x_1/(q^3x_0^3)$
+	-	+	-	-	+	-	-	+	+	-	+	$x_1/x_0$
+	-	+	-	-	+	+	-	+	-	-	+	$(x_0 - x_1)x_1/(qx_0^2)$
+	-	+	+	+	-	+	+	-	+	-	+	$x_1^2/x_0^2$
+	-	+	+	+	-	+	+	+	+	-	-	$(x_0 - x_1)x_1^2/(q^2x_0^3)$
+	-	+	+	-	+	+	-	+	+	-	+	$x_1^2/x_0^2$
+	-	+	-	+	+	-	+	+	+	-	+	$x_1^2/x_0^2$
+	-	+	-	+	+	+	+	+	-	-	+	$(x_0 - x_1)x_1^2/(qx_0^3)$
+	-	+	+	+	+	+	+	+	+	-	+	$x_1^3/x_0^3$
-	+	+	-	-	-	-	-	-	-	+	+	1
-	+	+	-	-	-	-	+	-	-	-	+	$(x_0 - x_1)/(qx_0)$
-	+	+	-	-	-	-	-	+	-	+	-	$(x_0 - x_1)/x_0$
-	+	+	-	-	-	-	+	+	-	-	-	$(q^2x_0 - x_1)(x_0 - x_1)/(q^2x_0^2)$
-	+	+	+	-	-	+	-	-	-	+	+	$x_1/x_0$
-	+	+	+	-	-	+	+	-	-	-	+	$(x_0 - x_1)x_1/(q^2x_0^2)$
-	+	+	+	-	-	+	-	+	-	+	-	$(x_0 - x_1)x_1/(qx_0^2)$
-	+	+	+	-	-	+	+	+	-	-	-	$(q^2x_0 - x_1)(x_0 - x_1)x_1/(q^4x_0^3)$
-	+	+	-	+	-	-	+	-	-	+	+	$x_1/x_0$
-	+	+	-	+	-	-	+	+	-	+	-	$(x_0 - x_1)x_1/(qx_0^2)$
-	+	+	-	-	+	-	-	+	-	+	+	$x_1/x_0$
-	+	+	-	-	+	-	+	+	-	-	+	$(x_0 - x_1)x_1/(qx_0^2)$
-	+	+	+	+	-	+	+	-	-	+	+	$x_1^2/x_0^2$
-	+	+	+	+	-	+	+	+	-	+	-	$(x_0 - x_1)x_1^2/(q^2x_0^3)$
-	+	+	+	-	+	+	-	+	-	+	+	$x_1^2/x_0^2$
-	+	+	+	-	+	+	+	+	-	-	+	$(x_0 - x_1)x_1^2/(q^2x_0^3)$
-	+	+	-	+	+	-	+	+	-	+	+	$x_1^2/x_0^2$
-	+	+	+	+	+	+	+	+	-	+	+	$x_1^3/x_0^3$
+	+	+	-	-	-	-	-	-	-	+	+	1
+	+	+	-	-	-	+	-	-	-	+	+	$(x_0 - x_1)/(q^2x_0)$
+	+	+	-	-	-	-	+	-	+	-	+	$(x_0 - x_1)/(qx_0)$
+	+	+	-	-	-	-	-	+	+	+	-	$(x_0 - x_1)/x_0$
+	+	+	-	-	-	+	+	-	-	-	+	$(q^2x_0 - x_1)(x_0 - x_1)/(q^4x_0^2)$
+	+	+	-	-	-	+	-	+	-	+	-	$(q^2x_0 - x_1)(x_0 - x_1)/(q^3x_0^2)$
+	+	+	-	-	-	-	+	+	+	-	-	$(q^2x_0 - x_1)(x_0 - x_1)/(q^2x_0^2)$
+	+	+	-	-	-	+	+	+	-	-	-	$(q^4x_0 - x_1)(q^2x_0 - x_1)(x_0 - x_1)/(q^6x_0^3)$
+	+	+	+	-	-	+	-	-	+	+	+	$x_1/x_0$
+	+	+	+	-	-	+	+	-	+	-	+	$(x_0 - x_1)x_1/(q^2x_0^2)$
+	+	+	+	-	-	+	-	+	+	+	-	$(x_0 - x_1)x_1/(qx_0^2)$
+	+	+	+	-	-	+	+	+	+	-	-	$(q^2x_0 - x_1)(x_0 - x_1)x_1/(q^4x_0^3)$
+	+	+	-	+	-	-	+	-	+	+	+	$x_1/x_0$
+	+	+	-	+	-	+	+	-	-	+	+	$(x_0 - x_1)x_1/(q^2x_0^2)$
+	+	+	-	+	-	-	+	+	+	+	-	$(x_0 - x_1)x_1/(qx_0^2)$
+	+	+	-	+	-	+	+	+	-	+	-	$(q^2x_0 - x_1)(x_0 - x_1)x_1/(q^4x_0^3)$
+	+	+	-	-	+	-	-	+	+	+	+	$x_1/x_0$

Continuation of Table 2												
$i_1$	$i_2$	$i_3$	$j_1$	$j_2$	$j_3$	$k_1$	$k_2$	$k_3$	$l_1$	$l_2$	$l_3$	weight
+	+	+	-	-	+	+	-	+	-	+	+	$(x_0 - x_1)x_1/(q^2x_0^2)$
+	+	+	-	-	+	-	+	+	+	-	+	$(x_0 - x_1)x_1/(qx_0^2)$
+	+	+	-	-	+	+	+	+	-	-	+	$(q^2x_0 - x_1)(x_0 - x_1)x_1/(q^4x_0^3)$
+	+	+	+	+	-	+	+	-	+	+	+	$x_1^2/x_0^2$
+	+	+	+	+	-	+	+	+	+	+	-	$(x_0 - x_1)x_1^2/(q^2x_0^3)$
+	+	+	+	-	+	+	-	+	+	+	+	$x_1^2/x_0^2$
+	+	+	+	-	+	+	+	+	+	-	+	$(x_0 - x_1)x_1^2/(q^2x_0^3)$
+	+	+	-	+	+	-	+	+	+	+	+	$x_1^2/x_0^2$
+	+	+	-	+	+	+	+	+	-	+	+	$(x_0 - x_1)x_1^2/(q^2x_0^3)$
+	+	+	+	+	+	+	+	+	+	+	+	$x_1^3/x_0^3$
End of Table												